Measurement of Energy Balances of Noble Gas-Hydrogen Discharge Plasmas Using Calvet Calorimetry

R. Mills, J. Dong, W. Good, P. Ray, J. He, B. Dhandapani

BlackLight Power, Inc.
493 Old Trenton Road
Cranbury, NJ 08512

From a solution of a Schrödinger-type wave equation with a nonradiative boundary condition based on Maxwell's equations, Mills predicts that atomic hydrogen may undergo a catalytic reaction with certain gaseous ions such as Ar^+ which ionize at integer multiples of the potential energy of atomic hydrogen, $27.2\,eV$. The reaction involves a nonradiative energy transfer to form a hydrogen atom that is lower in energy than unreacted atomic hydrogen with the release of energy. Upon the addition of 5% argon catalyst to a hydrogen plasma, the Lyman α emission was observed to increase by about an order of magnitude which indicated an increase in the plasma temperature; whereas, xenon control had no effect. Thus, the energy balances of argon-hydrogen glow discharge plasmas were measured using Calvet calorimetry. The steady state Calvet voltage significantly increased upon the addition of 3% hydrogen to an argon plasma, and the output signal was integrated until the signal returned to baseline. An energy balance of over $-151{,}000\,kJ/mole\,H_2$ was measured compared to the enthalpy of combustion of hydrogen of $-241.8\,kJ/mole\,H_2$. Whereas, under identical conditions no change in the Calvet voltage was observed when hydrogen was added to a plasma of xenon which does not provide a reaction with a net enthalpy of a multiple of the potential energy of atomic hydrogen under these conditions.

I. INTRODUCTION

A. Background

J. J. Balmer showed in 1885 that the frequencies for some of the lines observed in the emission spectrum of atomic hydrogen could be expressed with a completely empirical relationship. This approach was later extended by J. R. Rydberg, who showed that all of the spectral lines of atomic hydrogen were given by the equation:

$$\bar{\nu} = R\left(\frac{1}{n_f^2} - \frac{1}{n_i^2}\right) \tag{1}$$

where $R = 109{,}677\ cm^{-1}$, $n_f = 1,2,3,...$, $n_i = 2,3,4,...$, *and* $n_i > n_f$.

Niels Bohr, in 1913, developed a theory for atomic hydrogen that gave energy levels in agreement with Rydberg's equation. An identical equation, based on a totally different theory for the hydrogen atom, was developed by E. Schrödinger, and independently by W. Heisenberg, in 1926.

$$E_n = -\frac{e^2}{n^2 8\pi\varepsilon_o a_H} = -\frac{13.598\ eV}{n^2} \tag{2a}$$

$$n = 1,2,3,... \tag{2b}$$

where a_H is the Bohr radius for the hydrogen atom ($52.947\ pm$), e is the magnitude of the charge of the electron, and ε_o is the vacuum permittivity. Based on the solution of a Schrödinger-type wave equation with a nonradiative boundary condition based on Maxwell's equations, Mills [1-35] predicts that atomic hydrogen may undergo a catalytic reaction with certain atomized elements or certain gaseous ions which singly or multiply ionize at integer multiples of the potential energy of atomic hydrogen, $27.2\ eV$. The reaction involves a nonradiative energy transfer to form a hydrogen atom that is lower in energy than unreacted atomic hydrogen that corresponds to a fractional principal quantum number where Eq. (2b) should be replaced by Eq. (2c).

$$n = 1,2,3,...,\ and,\ n = \frac{1}{2},\frac{1}{3},\frac{1}{4},... \tag{2c}$$

A number of independent experimental observations lead to the conclusion that atomic hydrogen can exist in fractional quantum states that are at lower energies than the traditional "ground" ($n=1$) state.

B. Lower-Energy Hydrogen Experimental Data

Prior related studies that support the possibility of a novel reaction of atomic hydrogen which produces a chemically generated or assisted plasma (rt-plasma) and produces novel hydride compounds include extreme ultraviolet (EUV) spectroscopy [6-9, 11-18, 21-23], characteristic emission from catalysis and the hydride ion products [9-14], lower-energy hydrogen emission [4, 6, 7-8, 17], plasma formation [9, 11-16, 21-22, 24-25], Balmer α line broadening [7, 9, 11, 15-19], elevated electron temperature [7, 17], anomalous plasma afterglow duration [24-25], power generation [7, 9, 15-17, 19-21, 32], and analysis of chemical compounds [26-32]. Exemplary studies include:

1.) the observation of intense extreme ultraviolet (EUV) emission at low temperatures (e.g. $\approx 10^3\ K$) from atomic hydrogen and only those atomized elements or gaseous ions which provide a net enthalpy of reaction of approximately $m \cdot 27.2\ eV$ via the ionization of t electrons to a continuum energy level where t and m are each an integer (e.g. K, Cs, and Sr atoms and Rb^+ ion ionize at integer multiples of the potential energy of atomic hydrogen and caused emission; whereas, the chemically similar atoms, Na, Mg, and Ba, do not ionize at integer multiples of the potential energy of atomic hydrogen and caused no emission) [9, 11-16, 21-22, 24-25],

2.) the observation of novel EUV emission lines from microwave and glow discharges of helium with 2% hydrogen with energies of $q \cdot 13.6\ eV$ where $q = 1,2,3,4,6,7,8,9,11,12$ or these lines inelastically scattered by helium atoms in the excitation of $He(1s^2)$ to $He(1s^1 2p^1)$ that were identified as hydrogen transitions to electronic energy levels below the "ground" state corresponding to fractional quantum numbers [6, 7, 17],

3.) the observation of novel EUV emission lines from microwave and glow discharges of helium with 2% hydrogen at $44.2\ nm$ and $40.5\ nm$ with energies of $q \cdot 13.6 + \left(\frac{1}{n_f^2} - \frac{1}{n_i^2}\right) X 13.6\ eV$ where $q = 2$ and $n_f = 2,4$ $n_i = \infty$

that corresponded to multipole coupling to give two photon emission from a continuum excited state atom and an atom undergoing fractional Rydberg state transition [7],

4.) the identification of transitions of atomic hydrogen to lower energy levels corresponding to lower-energy hydrogen atoms in the extreme ultraviolet emission spectrum from interstellar medium and the sun [1, 4, 6, 8],

5.) the EUV spectroscopic observation of lines by the Institut für Niedertemperatur-Plasmaphysik e.V. that could be assigned to transitions of atomic hydrogen to lower energy levels corresponding to fractional principal quantum numbers and the emission from the excitation of the corresponding hydride ions [23],

6.) the recent analysis of mobility and spectroscopy data of individual electrons in liquid helium which shows direct experimental confirmation that electrons may have fractional principal quantum energy levels [5],

7.) the observation of novel EUV emission lines from microwave discharges of argon or helium with 10% hydrogen that matched those predicted for vibrational transitions of $H_2^*[n=1/4;n^*=2]^+$ with energies of $v \cdot 1.185\,eV$, $v=17$ *to* 38 that terminated at the predicted dissociation limit, E_D, of $H_2[n=1/4]^+$, $E_D=42.88\,eV\,(28.92\,nm)$ [8],

8.) the observation of continuum state emission of Cs^{2+} and Ar^{2+} at $53.3\,nm$ and $45.6\,nm$, respectively, with the absence of the other corresponding Rydberg series of lines from these species which confirmed the resonant nonradiative energy transfer of $27.2\,eV$ from atomic hydrogen to the catalysts atomic Cs or Ar^+ [14],

9.) the spectroscopic observation of the predicted hydride ion $H^-(1/2)$ of hydrogen catalysis by either Cs atom or Ar^+ catalyst at $407\,nm$ corresponding to its predicted binding energy of $3.05\,eV$ [14],

10.) the observation of $H^-(1/2)$, the hydride ion catalyst product of K^+/K^+ or Rb^+, by high resolution visible spectroscopy as a broad peak at $407.00\,nm$ with a FWHM of $0.14\,nm$ corresponding to its predicted binding energy of $3.0468\,eV$ [11],

11.) the observation that the high resolution visible plasma emission spectra in the region of $400.0\,nm$ to $406.0\,nm$ matched the predicted bound-free hyperfine structure lines E_{HF} of $H^-(1/2)$ calculated

from the electron g factor as $E_{HF} = j^2 3.0056\, X\, 10^{-5} + 3.0575\, eV$ (j is an integer) for $j = 1$ to $j = 37$ [16] to within a 1 part per 10^5 [11],

12.) the observation of characteristic emission from K^{3+} which confirmed the resonant nonradiative energy transfer of $3 \cdot 27.2\, eV$ from atomic hydrogen to atomic K [13],

13.) the spectroscopic observation of the predicted $H^-(1/4)$ ion of hydrogen catalysis by K catalyst at $110\, nm$ corresponding to its predicted binding energy of $11.2\, eV$ [11, 13],

14.) the observation of characteristic emission from Rb^{2+} which confirmed the resonant nonradiative energy transfer of $27.2\, eV$ from atomic hydrogen to Rb^+ [12],

15.) the spectroscopic observation of the predicted $H^-(1/2)$ ion of hydrogen catalysis by Rb^+ catalyst at $407\, nm$ corresponding to its predicted binding energy of $3.05\, eV$ [12],

16.) the observation by the Institut für Niedertemperatur-Plasmaphysik e.V. of an anomalous plasma and plasma afterglow duration formed with hydrogen-potassium mixtures [24],

17.) the observation of anomalous afterglow durations of plasmas formed by catalysts providing a net enthalpy of reaction within thermal energies of $m \cdot 27.28\, eV$ [24-25],

18.) the observation of Lyman series in the EUV that represents an energy release about 10 times that of hydrogen combustion which is greater than that of any possible known chemical reaction [9, 11-16, 21-22, 24-25],

19.) the observation of line emission by the Institut für Niedertemperatur-Plasmaphysik e.V. with a 4° grazing incidence EUV spectrometer that was 100 times more energetic than the combustion of hydrogen [23],

20.) the observation of anomalous plasmas formed with Sr and Ar^+ catalysts at 1% of the theoretical or prior known voltage requirement with a light output per unit power input up to 8600 times that of the control standard light source [15-16, 20-21],

21.) the observation that the optically measured output power of gas cells for power supplied to the glow discharge increased by over two orders of magnitude depending on the presence of less than 1% partial pressure of certain catalysts in hydrogen gas or argon-hydrogen gas

mixtures, and an excess thermal balance of 42 W was measured for the 97% argon and 3% hydrogen mixture versus argon plasma alone [20],

22.) the observation that glow discharge plasmas of the catalyst-hydrogen mixtures of strontium-hydrogen, helium-hydrogen, argon-hydrogen, strontium-helium-hydrogen, and strontium-argon-hydrogen showed significant Balmer α line broadening corresponding to an average hydrogen atom temperature of 25-45 eV; whereas, plasmas of the noncatalyst-hydrogen mixtures of pure hydrogen, krypton-hydrogen, xenon-hydrogen, and magnesium-hydrogen showed no excessive broadening corresponding to an average hydrogen atom temperature of $\approx 3\ eV$ [17-19],

23.) the observation that microwave helium-hydrogen and argon-hydrogen plasmas having catalyst Ar^+ or He^{2+} showed extraordinary Balmer α line broadening due to hydrogen catalysis corresponding to an average hydrogen atom temperature of 110-130 eV and 180-210 eV, respectively; whereas, plasmas of pure hydrogen, neon-hydrogen, krypton-hydrogen, and xenon-hydrogen showed no excessive broadening corresponding to an average hydrogen atom temperature of $\approx 3\ eV$ [7, 18],

24.) the observation that microwave helium-hydrogen and argon-hydrogen plasmas showed average electron temperatures that were high, 28,000 K and 11,600 K, respectively; whereas, the corresponding temperatures of helium and argon alone were only 6800 K and 4800 K, respectively [7, 18],

25.) the observation of significant Balmer α line broadening of 17, 9, 11, 14, *and* 24 eV from rt-plasmas of incandescently heated hydrogen with K^+/K^+, Rb^+, cesium, strontium, and strontium with Ar^+ catalysts, respectively, wherein the results could not be explained by Stark or thermal broadening or electric field acceleration of charged species since the measured field of the incandescent heater was extremely weak, 1 V/cm, corresponding to a broadening of much less than 1 eV [9],

26.) calorimetric measurement of excess power of 20 mW/cc on rt-plasmas formed by heating hydrogen with K^+/K^+ and Ar^+ as catalysts [9],

27.) the high resolution visible spectroscopic observation from rt-plasmas and plasma electrolysis cells of the predicted $H^-(1/2)$ ion of hydrogen catalysis by each of K^+/K^+, Rb^+, Cs, and Ar^+ at 407 nm corresponding to its predicted binding energy of 3.05 eV [9-11],

28.) the isolation of novel inorganic hydride compounds such as $KH\,KHCO_3$ and KH following each of the electrolysis and plasma electrolysis of a K_2CO_3 electrolyte which comprised high binding energy hydride ions that were stable in water with their identification by methods such as (i) ToF-SIMS on $KH\,KHCO_3$ which showed inorganic hydride clusters $K[KH\,KHCO_3]_n^+$ and a negative ToF-SIMS dominated by hydride ion, (ii) X-ray photoelectron spectroscopy which showed novel peaks corresponding to high binding energy hydride ions, and (iii) proton nuclear magnetic resonance spectroscopy which showed upfield shifted peaks corresponding to more diamagnetic, high-binding-energy hydride ions [10, 28-29, 31],

29.) the observation that the power output exceeded the power supplied to a hydrogen glow discharge plasmas by 35-184 W depending on the presence of catalysts from helium or argon and less than 1% partial pressure of strontium metal in noble gas-hydrogen mixtures; whereas, the chemically similar noncatalyst krypton had no effect on the power balance [19],

30.) the observation that upon the addition of 10% hydrogen to a helium microwave plasma maintained with a constant microwave input power of $40\,W$, the thermal output power was measured to be at least $400\,W$ corresponding to a reactor temperature rise from room temperature to 1200 °C within 150 seconds, a power density of $40\,MW/m^3$, and an energy balance of at least $-5\,X\,10^5\,kJ/mole\,H_2$ compared to the enthalpy of combustion of hydrogen of $-241.8\,kJ/mole\,H_2$ [17],

31.) the differential scanning calorimetry (DSC) measurement of minimum heats of formation of KHI by the catalytic reaction of K with atomic hydrogen and KI that were over $-2000\,kJ/mole\,H_2$ compared to the enthalpy of combustion of hydrogen of $-241.8\,kJ/mole\,H_2$ [32],

32.) the isolation of novel hydrogen compounds as products of the reaction of atomic hydrogen with atoms and ions which formed an anomalous plasma as reported in the EUV studies [26-32],

33.) the identification of novel hydride compounds by a number of analytic methods as such as (i) time of flight secondary ion mass spectroscopy which showed a dominant hydride ion in the negative ion spectrum, (ii) X-ray photoelectron spectroscopy which showed novel hydride peaks and significant shifts of the core levels of the primary

elements bound to the novel hydride ions, (iii) ^1H nuclear magnetic resonance spectroscopy (NMR) which showed extraordinary upfield chemical shifts compared to the NMR of the corresponding ordinary hydrides, and iv.) thermal decomposition with analysis by gas chromatography, and mass spectroscopy which identified the compounds as hydrides [26-32],

34.) the NMR identification of novel hydride compounds MH^*X wherein M is the alkali or alkaline earth metal, X, is a halide, and H^* comprises a novel high binding energy hydride ion identified by a large distinct upfield resonance [26-31],

35.) the replication of the NMR results of the identification of novel hydride compounds by large distinct upfield resonances at Spectral Data Services, University of Massachusetts Amherst, University of Delaware, Grace Davison, and National Research Council of Canada [26],

36.) the NMR identification of novel hydride compounds MH^* and MH_2^* wherein M is the alkali or alkaline earth metal and H^* comprises a novel high binding energy hydride ion identified by a large distinct upfield resonance that proves the hydride ion is different from the hydride ion of the corresponding known compound of the same composition [26].

C. Mechanism of the Formation of Lower-Energy Atomic Hydrogen

The mechanism of the EUV emission, the formation of novel hydrides, and the observation of certain EUV lines from interstellar medium and the sun can not be explained by the conventional energy levels of hydrogen, but it is predicted by a solution of the Schrödinger equation with a nonradiative boundary constraint put forward by Mills [1]. Mills predicts that certain atoms or ions serve as catalysts to release energy from hydrogen to produce an increased binding energy hydrogen atom called a *hydrino atom* having a binding energy given by Eq. (2a) where

$$n = \frac{1}{2}, \frac{1}{3}, \frac{1}{4}, \ldots, \frac{1}{p} \tag{3}$$

and p is an integer greater than 1, designated as $H\left[\frac{a_H}{p}\right]$ where a_H is the radius of the hydrogen atom. Hydrinos are predicted to form by reacting an ordinary hydrogen atom with a catalyst having a net enthalpy of reaction of about

$$m \cdot 27.2\ eV \tag{4}$$

where m is an integer. This catalysis releases energy from the hydrogen atom with a commensurate decrease in size of the hydrogen atom, $r_n = na_H$. For example, the catalysis of $H(n=1)$ to $H(n=1/2)$ releases $40.8\ eV$, and the hydrogen radius decreases from a_H to $\frac{1}{2}a_H$.

The excited energy states of atomic hydrogen are also given by Eq. (2a) except with Eq. (2b). The $n=1$ state is the "ground" state for "pure" photon transitions (the $n=1$ state can absorb a photon and go to an excited electronic state, but it cannot release a photon and go to a lower-energy electronic state). However, an electron transition from the ground state to a lower-energy state is possible by a nonradiative energy transfer such as multipole coupling or a resonant collision mechanism. These lower-energy states have fractional quantum numbers, $n=\frac{1}{\text{integer}}$. Processes that occur without photons and that require collisions are common. For example, the exothermic chemical reaction of $H+H$ to form H_2 does not occur with the emission of a photon. Rather, the reaction requires a collision with a third body, M, to remove the bond energy- $H+H+M \rightarrow H_2+M^*$ [36]. The third body distributes the energy from the exothermic reaction, and the end result is the H_2 molecule and an increase in the temperature of the system. Some commercial phosphors are based on nonradiative energy transfer involving multipole coupling. For example, the strong absorption strength of Sb^{3+} ions along with the efficient nonradiative transfer of excitation from Sb^{3+} to Mn^{2+} are responsible for the strong manganese luminescence from phosphors containing these ions [37].

Similarly, the $n=1$ state of hydrogen and the $n=\frac{1}{\text{integer}}$ states of hydrogen are nonradiative, but a transition between two nonradiative states, say $n=1$ to $n=1/2$, is possible via a nonradiative energy transfer. In these cases, during the transition the electron couples to another

electron transition, electron transfer reaction, or inelastic scattering reaction which can absorb the exact amount of energy that must be removed from the hydrogen atom to cause the transition. Thus, a catalyst provides a net positive enthalpy of reaction of $m \cdot 27.2\ eV$ (i.e. it absorbs $m \cdot 27.2\ eV$ where m is an integer). Certain atoms or ions serve as catalysts by accepting energy from hydrogen atoms through a nonradiative resonant transfer. The catalyst may then release the transferred energy by radiative and nonradiative mechanisms. As a consequence of the nonradiative energy transfer, the hydrogen atom becomes unstable and emits further energy until it achieves a lower-energy nonradiative state having a principal energy level given by Eqs. (2a) and (3).

D. Catalysts

Argon ions can provide a net enthalpy of a multiple of that of the potential energy of the hydrogen atom. The second ionization energy of argon is $27.63\ eV$ [38]. The reaction Ar^+ to Ar^{2+} has a net enthalpy of reaction of $27.63\ eV$, which is equivalent to $m=1$ in Eq. (4).

$$27.63\ eV + Ar^+ + H\left[\frac{a_H}{p}\right] \rightarrow Ar^{2+} + e^- + H\left[\frac{a_H}{(p+1)}\right] + [(p+1)^2 - p^2]X13.6\ eV \tag{5}$$

$$Ar^{2+} + e^- \rightarrow Ar^+ + 27.63\ eV \tag{6}$$

And, the overall reaction is

$$H\left[\frac{a_H}{p}\right] \rightarrow H\left[\frac{a_H}{(p+1)}\right] + [(p+1)^2 - p^2]X13.6\ eV \tag{7}$$

The energy given off during catalysis is much greater than the energy lost to the catalyst. The energy released is large compared to conventional chemical reactions. For example, when hydrogen and oxygen gases undergo combustion to form water

$$H_2(g) + \frac{1}{2}O_2(g) \rightarrow H_2O(g) \tag{8}$$

the known enthalpy of formation of water is $\Delta H_f = -241.8\ kJ/mole$ or 1.25 eV per hydrogen atom. By contrast, each $(n=1)$ ordinary hydrogen atom undergoing catalysis releases a net of $40.8\ eV$. Moreover, further catalytic transitions may occur: $n=\frac{1}{2} \rightarrow \frac{1}{3}$, $\frac{1}{3} \rightarrow \frac{1}{4}$, $\frac{1}{4} \rightarrow \frac{1}{5}$, and so on. Once catalysis

begins. hydrinos autocatalyze further in a process called *disproportionation*. This mechanism is similar to that of an inorganic ion catalysis. But, hydrino catalysis should have a higher reaction rate than that of the inorganic ion catalyst due to the better match of the enthalpy to $m \cdot 27.2\ eV$.

II. EXPERIMENTAL

A. EUV Spectroscopy

Extreme ultraviolet (EUV) spectroscopy was recorded on a hydrogen microwave plasma alone and with 5% argon or 5% xenon. Due to the extremely short wavelength of this radiation, "transparent" optics do not exist. Therefore, a windowless arrangement was used wherein the microwave discharge cell was connected to the same vacuum vessel as the grating and detectors of the EUV spectrometer. Differential pumping permitted a high pressure in the cell as compared to that in the spectrometer. This was achieved by pumping on the cell outlet and pumping on the grating side of the collimator that served as a pin-hole inlet to the optics. The spectrometer was continuously evacuated to $10^{-4} - 10^{-6}$ Torr by a turbomolecular pump with the pressure read by a cold cathode pressure gauge. The EUV spectrometer was connected to the cell light source with a 1.5 mm X 5 mm collimator which provided a light path to the slits of the EUV spectrometer. The collimator also served as a flow constrictor of gas from the cell. The cell was operated under gas flow conditions while maintaining a constant gas pressure in the cell.

For spectral measurement, the light emission from microwave plasmas of hydrogen alone, hydrogen-argon (95/5%), and hydrogen-xenon (95/5%) were introduced to a normal incidence McPherson 0.2 meter monochromator (Model 302, Seya-Namioka type) equipped with a 1200 lines/mm holographic grating with a platinum coating. The wavelength region covered by the monochromator was $5 - 560\ nm$. The UV spectrum ($90 - 165\ nm$) of the cell emission was recorded with a photomultiplier tube (PMT) and a sodium salicylate scintillator. The PMT (Model R1527P, Hamamatsu) used has a spectral response in the range of $185 - 680\ nm$ with a peak efficiency at about $400\ nm$. The wavelength

resolution was about 1 nm (FWHM) with an entrance and exit slit width of 300 μm. The increment was 0.1 nm and the dwell time was 500 ms.

B. Microwave Emission Spectra

The experimental set up comprising a microwave discharge gas cell light source and an EUV spectrometer which was differentially pumped is shown in Figure 1. Extreme ultraviolet emission spectra were obtained on plasmas of hydrogen alone, hydrogen-argon mixture (95/5%), and hydrogen-xenon mixture (95/5%). Hydrogen or the hydrogen-noble gas mixture was flowed through a half inch diameter quartz tube at 1 Torr that was maintained by flowing hydrogen or the gas mixture while monitoring the pressure with a 10 Torr and 1000 Torr MKS Baratron absolute pressure gauge. The tube was fitted with an Opthos coaxial microwave cavity (Evenson cavity). The microwave generator was a Opthos model MPG-4M generator (Frequency: 2450 MHz). The input power to the plasma was set at 85 watts. The EUV spectrometer was a normal incidence monochromator. (See EUV-Spectroscopy Section).

C. Calvet Calorimeter Methods

The instrument used to measure the heat of reaction was a cylindrical heat flux calorimeter (International Thermal Instrument Co., Model CA-100-1). The cylindrical calorimeter walls contained a thermopile structure composed of two sets of thermoelectric junctions. One set of junctions was in thermal contact with the internal calorimeter wall, at temperature T_i, and the second set of thermal junctions was in thermal contact with the external calorimeter wall at T_e which was held constant by a forced convection oven. When heat was generated in the calorimeter cell, the calorimeter radially transferred a constant fraction of this heat into the surrounding heat sink. As heat flowed a temperature gradient, $(T_i - T_e)$, was established between the two sets of thermopile junctions. This temperature gradient generated a voltage which was compared to the linear voltage versus power calibration curve to give the power of reaction. The calorimeter was calibrated with a precision resistor and a fixed current source at power levels

representative of the power of reaction of the catalyst runs. At constant total pressure, the calibration constant of the Calvet calorimeter was not sensitive to the flow of test gas over the range of conditions of the tests. To avoid corrosion, a cylindrical reactor, machined from 304 stainless steel to fit inside the calorimeter, was used to contain the reaction. To maintain an isothermal reaction system and improve baseline stability, the calorimeter was placed inside a commercial forced convection oven (Precision Scientific 625 S) that was operated at room temperature to $475\,K$. A more complete description of a similar instrument and methods are given by Bradford, Phillips, and Klanchar [39]. The general system design of the Calvet calorimeter is shown in Figure 2.

D. Gas Cell for Calvet Calorimeter

The cylindrical stainless steel gas discharge cell and Calvet instrument for plasma energy balance studies with argon with 3% hydrogen addition compared to xenon with 3% hydrogen addition is shown in Figure 3. The cell comprised a 800 cm^3 stainless steel vessel capable of containing a vacuum or a pressure above atmospheric. The cell was maintained at an elevated isothermal temperature by a forced convection oven. The operating temperature of the gas cell was $475\,K$. The cell was used in the vertical position and was inserted into a thermopile. The flange was sealed with a silver plated copper gasket. The flange had a centered high voltage feedthrough which transmitted the power, supplied through a power connector, to a hollow cathode inside the cell. The axial hollow cathode glow discharge electrode assembly shown in Figure 3 comprised a stainless steel plate (4.2 cm diameter, 0.9 mm thick) anode and a circumferential stainless steel cylindrical frame (5.1 cm OD, 7.2 cm long) perforated with evenly spaced 1 cm diameter holes. The cathode was wound with several layers of nickel screen and was attached to the cell body by a stainless steel wire covered with ceramic beads for electrical insulation, and the cell body was grounded. The flange also had a 1/4" vacuum port through which a 1/8" inlet for argon, krypton, xenon, or hydrogen passed. The 1/8" inlet was connected to a 1/4" stainless steel tube which connected to a Tee, a needle valve, a pressure gauge, and noble gas and hydrogen supplies.

The elbow port of the Tee was attached to a vacuum gauge, a needle valve, and then a vacuum pump.

The gas in each experiment was ultrahigh pure grade or higher (Praxair). Test gases comprised hydrogen alone, krypton alone, xenon alone, xenon with the initial addition of 3% hydrogen, argon alone, and argon with the initial addition of 3% hydrogen. In the case of calibration experiments, the steady state Calvet voltage output was recorded as the power was varied over the power range of 10 W to 100 W for plasmas of pure hydrogen, krypton, or xenon at 3 Torr.

In the case of energy balance measurements, the noble gas pressure inside the cell was maintained at 3 Torr under static discharge conditions. After the calorimeter reached a steady state with 20 W of input power to the plasma, the total pressure was reduced by pumping, and hydrogen was added until the total pressure was 3 Torr for an initial noble gas-hydrogen mixture of 97/3%. Each gas flow was controlled by a 0-20 sccm range mass flow controller (MKS 1179A21CS1BB) with a readout (MKS type 246). The cell pressure was monitored by a 0-10 Torr MKS Baratron absolute pressure gauge. After achieving the desired gas mixture, the cell was run static with the input power unchanged. The Calvet output voltage was recorded as the hydrogen was consumed as indicated by a 3% drop in pressure as the elevated signal returned to baseline. No exotherm or pressure drop was observed in the case of xenon-hydrogen; so, the experiment was recorded for the same period of time as the argon-hydrogen experiment. The data was recorded with a PC based computer data acquisition system (National Instruments).

E. Energy balance measurements

Since the ambient temperature was held constant, the general form of the energy balance equation for the cell in steady state is:

$$0 = P_{in} + P_{ex} - P_{loss} \tag{9}$$

where P_{in} is the input power to the discharge, P_{ex} is the excess power generated from the hydrogen catalysis reaction, and P_{loss} is the thermal power loss from the cell. The Calvet voltage response to input power for hydrogen, krypton, or xenon alone was determined over the constant input power range of 10 W to 100 W. The data was recorded after the

cell had reached a thermal steady state with each increase in the input power to the glow discharge which typically occurred in 20 hours. At this point, the power lost from the cell P_{loss} was equal to the total power P_T supplied to the cell P_{in} plus any excess power P_{ex}.

$$P_T = P_{in} + P_{ex} = P_{loss} \tag{10}$$

Since the heat transfer was dominated by conduction, the output voltage of the cell V was modeled by a linear curve

$$V = aP_T + C \tag{11}$$

where a and C are constants for the least square curve fit of the Calvet voltage response to power input for the control experiments ($P_{ex} = 0$). V was recorded as a function of input power P_{in} for noncatalyst controls as the input power was varied. The higher voltage produced by the catalyst gas with hydrogen compared with the control gases was representative of the excess power. In the case of the catalyst run, the total output power P_T was determined by solving Eq. (11) using the measured V. The excess power P_{ex} was determined from Eq. (10). The integral of the excess power P_{ex} over time gave the excess energy E_{ex}.

III. RESULTS

A. Argon-hydrogen microwave emission spectrum

The EUV spectrum ($90-165\,nm$) of the cell emission from the hydrogen plasma (dotted line) and the hydrogen plasma to which 5% argon was added (solid line) is shown in Figure 4. Upon the addition of 5% argon, the hydrogen Lyman α emission intensity was observed to increase by about an order of magnitude which is indicative of a higher plasma temperature. Essentially no effect was observed for the addition of 5% xenon to the hydrogen plasma.

B. Power balance measurements

The Calvet voltage as a function of the power applied to each of the control gases at 3 Torr total pressure was plotted for the input power range of 10 W to 100 W as shown in Figure 5. The least squares fit of the V response to unit input power calculated from the control plasmas,

hydrogen, krypton, or xenon alone, (Eq. (11)) was determined to be

$$V = 7.93 + 2.25 \times P_T \quad (12)$$

An argon plasma was maintained at a constant 20 W input power until steady state. The Calvet voltage significantly increased upon the addition of 3% hydrogen, and the output signal was recorded until the signal returned to baseline as shown in Figure 6. Due to the long response time of the Calvet calorimeter (20 hours), the result shown in Figure 6 was essentially the Calvet impulse response. The excess power was determine from Eq. (12) and Eq. (10). The integral of the power over the exotherm gave an energy balance of $-151{,}000\ kJ/mole\ H_2$. The experiment was repeated for xenon. The addition of hydrogen did not produce an exotherm as shown in Figure 7.

IV. DISCUSSION

Upon the addition of 5% argon to a hydrogen plasma, the Lyman alpha emission was observed to increase by about an order of magnitude which indicated an increase in the plasma temperature; whereas, no effect was observed with xenon. Thus, the energy balances of argon-hydrogen glow discharge plasmas were measured using Calvet calorimetry. The steady state Calvet voltage significantly increased upon the addition of 3% hydrogen, and the output signal was integrated until the signal returned to baseline. Energy balances of over $-151{,}000\ kJ/mole\ H_2$ were measured compared to the enthalpy of combustion of hydrogen of $-241.8\ kJ/mole\ H_2$. Whereas, under identical conditions no change in the Calvet voltage was observed when hydrogen was added to a plasma of xenon.

Argon is a source of the catalyst, Ar^+; whereas, xenon does not provide a reaction with a net enthalpy of a multiple of the potential energy of atomic hydrogen under these conditions. The presently observed energy balances were about $785\ eV/H\ atom$. The results indicate that once a hydrino atom is formed by a catalyst (Eqs. (5-7)) further catalytic transitions: $n=\frac{1}{2} \rightarrow \frac{1}{3}$, $\frac{1}{3} \rightarrow \frac{1}{4}$, $\frac{1}{4} \rightarrow \frac{1}{5}$, and so on occur to a substantial extent. This is consistent with the previously reported series of lower-energy hydrogen lines with energies of $q \cdot 13.6\ eV$ where

q = 1,2,3,4,6,7,8,9,11,12 [6-7, 17] and the studies given in Section B of the Introduction which show very large energy balances.

Since the net enthalpy released may be over several hundred times that of combustion, the catalysis of atomic hydrogen represents a new source of energy with H_2O as the source of hydrogen fuel. Moreover, rather than air pollutants or radioactive waste, novel hydride compounds with potential commercial applications are the products [26-32]. Since the power is in the form of a plasma, direct high-efficiency, low cost energy conversion may be possible [33-35], thus, avoiding a heat engine such as a turbine or a reformer-fuel cell system. Significantly lower capital costs and lower commercial operating costs than that of any known competing energy source are anticipated.

REFERENCES

1. R. Mills, *The Grand Unified Theory of Classical Quantum Mechanics*, September 2001 Edition, BlackLight Power, Inc., Cranbury, New Jersey, Distributed by Amazon.com; posted at www.blacklightpower.com.
2. R. Mills, "The Grand Unified Theory of Classical Quantum Mechanics", Global Foundation, Inc. Orbis Scientiae entitled *The Role of Attractive and Repulsive Gravitational Forces in Cosmic Acceleration of Particles The Origin of the Cosmic Gamma Ray Bursts*, (29th Conference on High Energy Physics and Cosmology Since 1964) Dr. Behram N. Kursunoglu, Chairman, December 14-17, 2000, Lago Mar Resort, Fort Lauderdale, FL, Kluwer Academic/Plenum Publishers, New York, pp. 243-258.
3. R. Mills, "The Grand Unified Theory of Classical Quantum Mechanics", Int. J. of Hydrogen Energy, in press.
4. R. Mills, "The Hydrogen Atom Revisited", Int. J. of Hydrogen Energy, Vol. 25, Issue 12, December, (2000), pp. 1171-1183.
5. R. Mills, The Nature of Free Electrons in Superfluid Helium—a Test of Quantum Mechanics and a Basis to Review its Foundations and Make a Comparison to Classical Theory, Int. J. Hydrogen Energy, Vol. 26, No. 10, (2001), pp. 1059-1096.
6. R. Mills, P. Ray, "Spectral Emission of Fractional Quantum Energy Levels of Atomic Hydrogen from a Helium-Hydrogen Plasma and the Implications for Dark Matter", Int. J. Hydrogen Energy, in press.

7. R. L. Mills, P. Ray, B. Dhandapani, J. He, "Spectroscopic Identification of Fractional Rydberg States of Atomic Hydrogen" J. Phys. Chem. Letts., submitted.
8. R. Mills, P. Ray, "Vibrational Spectral Emission of Fractional-Principal-Quantum-Energy-Level Hydrogen Molecular Ion", Int. J. Hydrogen Energy, in press.
9. R. Mills, P. Ray, M. Nansteel, W. Good, P. Jansson, B. Dhandapani, J. He, "Excessive Balmer α Line Broadening, Power Balance, and Novel Hydride Ion Product of Plasma Formed from Incandescently Heated Hydrogen Gas with Certain Catalysts", Int. J. Hydrogen Energy, submitted.
10. R. Mills, E. Dayalan, P. Ray, B. Dhandapani, J. He, "Highly Stable Novel Inorganic Hydrides from Aqueous Electrolysis and Plasma Electrolysis, Japanese Journal of Applied Physics, submitted.
11. R. L. Mills, P. Ray, " High Resolution Spectroscopic Observation of the Bound-Free Hyperfine Levels of a Novel Hydride Ion Corresponding to a Fractional Rydberg State of Atomic Hydrogen", Int. J. Hydrogen Energy, submitted.
12. R. L. Mills, P. Ray, "Spectroscopic Identification of a Novel Catalytic Reaction of Rubidium Ion with Atomic Hydrogen and the Hydride Ion Product", Int. J. Hydrogen Energy, in press.
13. R. Mills, P. Ray, Spectroscopic Identification of a Novel Catalytic Reaction of Potassium and Atomic Hydrogen and the Hydride Ion Product, Int. J. Hydrogen Energy, Vol. 27, No. 2, February, (2002), pp. 183-192.
14. R. Mills, "Spectroscopic Identification of a Novel Catalytic Reaction of Atomic Hydrogen and the Hydride Ion Product", Int. J. Hydrogen Energy, Vol. 26, No. 10, (2001), pp. 1041-1058.
15. R. Mills and M. Nansteel, "Argon-Hydrogen-Strontium Plasma Light Source", IEEE Transactions on Plasma Science, submitted.
16. R. Mills, M. Nansteel, and Y. Lu, "Excessively Bright Hydrogen-Strontium Plasma Light Source Due to Energy Resonance of Strontium with Hydrogen", European Journal of Physics D, submitted.
17. R. L. Mills, P. Ray, B. Dhandapani, M. Nansteel, X. Chen, J. He, "New Power Source from Fractional Quantum Energy Levels of Atomic Hydrogen that Surpasses Internal Combustion", Spectrochimica Acta,

submitted.

18. R. L. Mills, P. Ray, B. Dhandapani, J. He, "Comparison of Excessive Balmer α Line Broadening of Glow Discharge and Microwave Hydrogen Plasmas with Certain Catalysts" Chem. Phys., submitted.
19. R. L. Mills, A. Voigt, P. Ray, M. Nansteel, B. Dhandapani, "Measurement of Hydrogen Balmer Line Broadening and Thermal Power Balances of Noble Gas-Hydrogen Discharge Plasmas", Int. J. Hydrogen Energy, in press.
20. R. Mills, N. Greenig, S. Hicks, "Optically Measured Power Balances of Anomalous Discharges of Mixtures of Argon, Hydrogen, and Potassium, Rubidium, Cesium, or Strontium Vapor", Int. J. Hydrogen Energy, in press.
21. R. Mills, M. Nansteel, and Y. Lu, "Observation of Extreme Ultraviolet Hydrogen Emission from Incandescently Heated Hydrogen Gas with Strontium that Produced an Anomalous Optically Measured Power Balance", Int. J. Hydrogen Energy, Vol. 26, No. 4, (2001), pp. 309-326.
22. R. Mills, J. Dong, Y. Lu, "Observation of Extreme Ultraviolet Hydrogen Emission from Incandescently Heated Hydrogen Gas with Certain Catalysts", Int. J. Hydrogen Energy, Vol. 25, (2000), pp. 919-943.
23. R. Mills, "Observation of Extreme Ultraviolet Emission from Hydrogen-KI Plasmas Produced by a Hollow Cathode Discharge", Int. J. Hydrogen Energy, Vol. 26, No. 6, (2001), pp. 579-592.
24. R. Mills, "Temporal Behavior of Light-Emission in the Visible Spectral Range from a Ti-K2CO3-H-Cell", Int. J. Hydrogen Energy, Vol. 26, No. 4, (2001), pp. 327-332.
25. R. Mills, T. Onuma, and Y. Lu, "Formation of a Hydrogen Plasma from an Incandescently Heated Hydrogen-Catalyst Gas Mixture with an Anomalous Afterglow Duration", Int. J. Hydrogen Energy, Vol. 26, No. 7, July, (2001), pp. 749-762.
26. R. Mills, B. Dhandapani, M. Nansteel, J. He, A. Voigt, "Identification of Compounds Containing Novel Hydride Ions by Nuclear Magnetic Resonance Spectroscopy", Int. J. Hydrogen Energy, Vol. 26, No. 9, Sept. (2001), pp. 965-979.
27. R. Mills, B. Dhandapani, N. Greenig, J. He, "Synthesis and Characterization of Potassium Iodo Hydride", Int. J. of Hydrogen Energy, Vol. 25, Issue 12, December, (2000), pp. 1185-1203.

28. R. Mills, "Novel Inorganic Hydride", Int. J. of Hydrogen Energy, Vol. 25, (2000), pp. 669-683.
29. R. Mills, "Novel Hydrogen Compounds from a Potassium Carbonate Electrolytic Cell", Fusion Technology, Vol. 37, No. 2, March, (2000), pp. 157-182.
30. R. Mills, B. Dhandapani, M. Nansteel, J. He, T. Shannon, A. Echezuria, "Synthesis and Characterization of Novel Hydride Compounds", Int. J. of Hydrogen Energy, Vol. 26, No. 4, (2001), pp. 339-367.
31. R. Mills, "Highly Stable Novel Inorganic Hydrides", Journal of New Materials for Electrochemical Systems, in press.
32. R. Mills, W. Good, A. Voigt, Jinquan Dong, "Minimum Heat of Formation of Potassium Iodo Hydride", Int. J. Hydrogen Energy, Vol. 26, No. 11, Oct., (2001), pp. 1199-1208.
33. R. Mills, "BlackLight Power Technology-A New Clean Hydrogen Energy Source with the Potential for Direct Conversion to Electricity", Proceedings of the National Hydrogen Association, 12 th Annual U.S. Hydrogen Meeting and Exposition, *Hydrogen: The Common Thread*, The Washington Hilton and Towers, Washington DC, (March 6-8, 2001), pp. 671-697.
34. R. Mills, "BlackLight Power Technology-A New Clean Energy Source with the Potential for Direct Conversion to Electricity", Global Foundation International Conference on "Global Warming and Energy Policy", Dr. Behram N. Kursunoglu, Chairman, Fort Lauderdale, FL, November 26-28, 2000, Kluwer Academic/Plenum Publishers, New York, pp. 1059-1096.
35. R. Mayo, R. Mills, M. Nansteel, "On the Potential of Direct and MHD Conversion of Power from a Novel Plasma Source to Electricity for Microdistributed Power Applications", IEEE Transactions on Plasma Science, submitted.
36. N. V. Sidgwick, *The Chemical Elements and Their Compounds*, Volume I, Oxford, Clarendon Press, (1950), p.17.
37. M. D. Lamb, *Luminescence Spectroscopy*, Academic Press, London, (1978), p. 68.
38. D. R. Linde, *CRC Handbook of Chemistry and Physics*, 79 th Edition, CRC Press, Boca Raton, Florida, (1998-9), p. 10-175 to p. 10-177.
39. M. C. Bradford, J. Phillips, J., Klanchar, Rev. Sci. Instrum., 66, (1),

January, (1995), pp. 171-175.

Figure Captions

Figure 1. The experimental set up comprising a microwave discharge gas cell light source and an EUV spectrometer which was differentially pumped.

Figure 2. The general system design of the Calvet calorimeter.

Figure 3. Cylindrical stainless steel gas discharge cell and Calvet instrument for plasma energy balance studies of argon with the addition of 3% hydrogen compared to xenon with the addition of 3% hydrogen.

Figure 4. The EUV spectrum ($90-165\,nm$) of the cell emission from the hydrogen plasma (dotted line) and the hydrogen plasma to which 5% argon was added (solid line).

Figure 5. The Calvet voltage of as a function of the input power applied to each of the control gases, hydrogen, krypton, and xenon alone, at 3 Torr total pressure was plotted for the input power range of 10 W to 100 W.

Figure 6. At constant input power, the Calvet signal response upon the switch of a 3 Torr argon plasma to plasma with 0.08 Torr of hydrogen and 2.92 Torr of argon. The integral of the power over the exotherm gave an energy balance of $-151{,}000\,kJ/mole\,H_2$.

Figure 7. At constant input power, the Calvet signal response upon the switch of a 3 Torr xenon plasma to plasma with 0.08 Torr of hydrogen and 2.92 Torr of xenon where no exotherm was observed.

Fig. 1

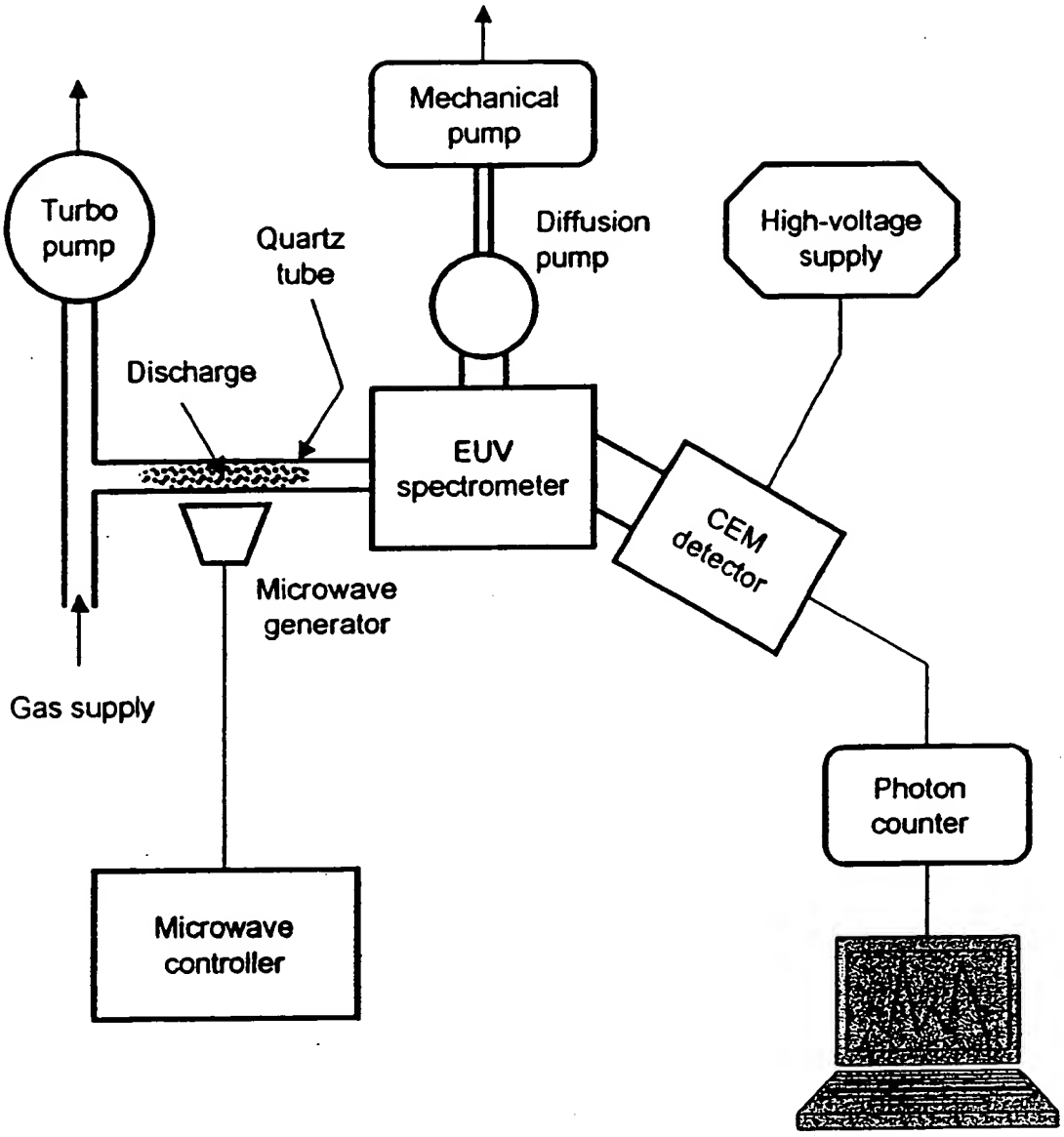
Mechanical pump
Turbo pump
Quartz tube
Diffusion pump
High-voltage supply
Discharge
EUV spectrometer
CEM detector
Microwave generator
Gas supply
Photon counter
Microwave controller

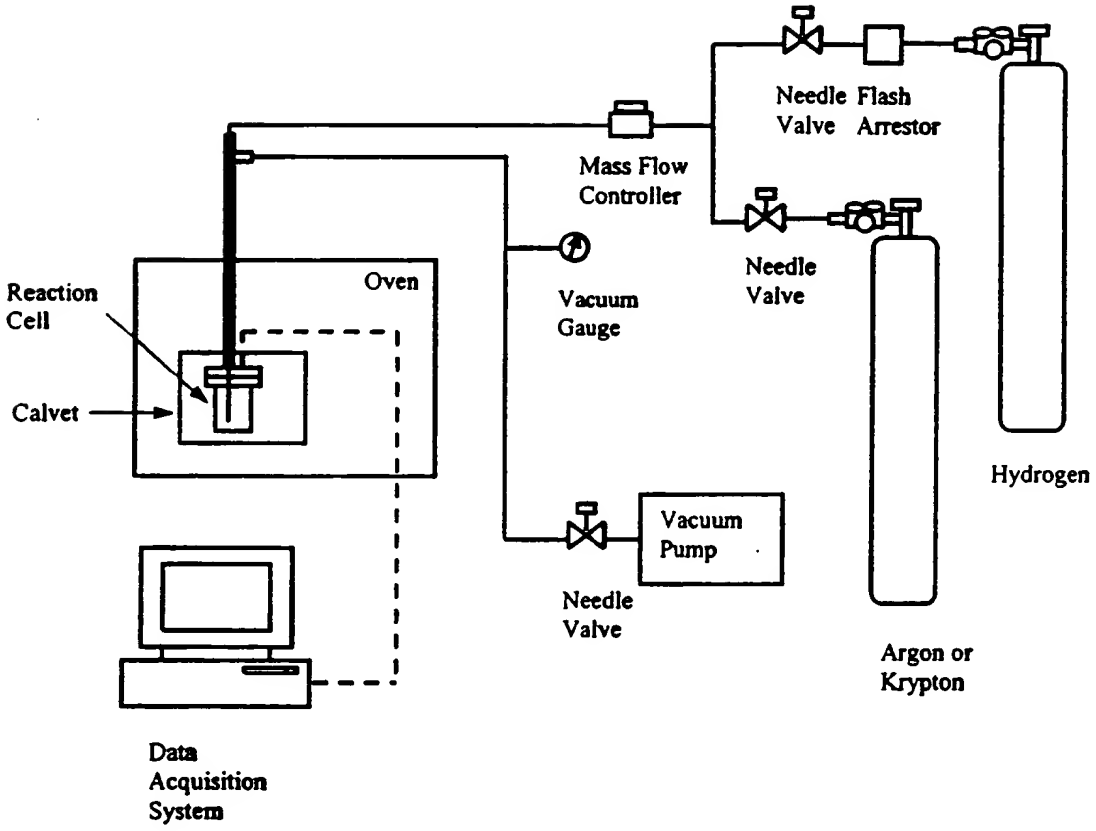
Needle Valve
Flash Arrestor
Mass Flow Controller
Needle Valve
Vacuum Gauge
Oven
Reaction Cell
Calvet
Hydrogen
Vacuum Pump
Needle Valve
Argon or Krypton
Data Acquisition System

Fig. 2

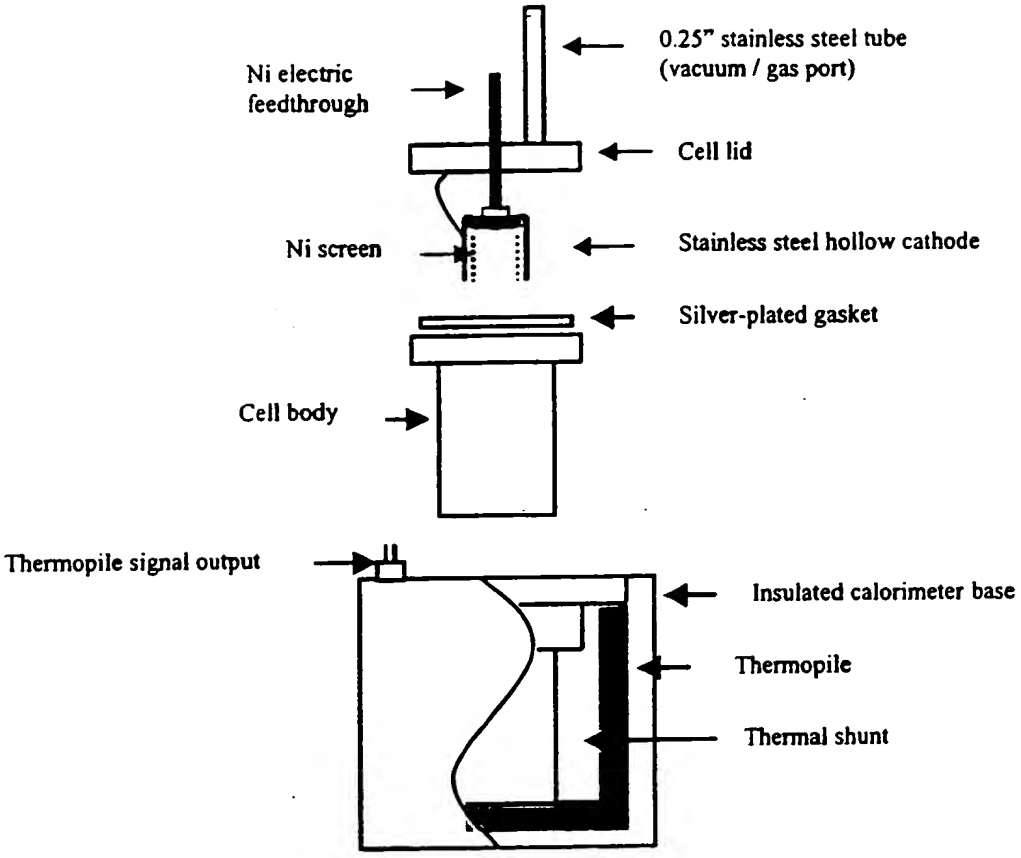
0.25" stainless steel tube
(vacuum / gas port)
Ni electric
feedthrough
Cell lid
Ni screen
Stainless steel hollow cathode
Silver-plated gasket
Cell body
Thermopile signal output
Insulated calorimeter base
Thermopile
Thermal shunt

Fig. 3

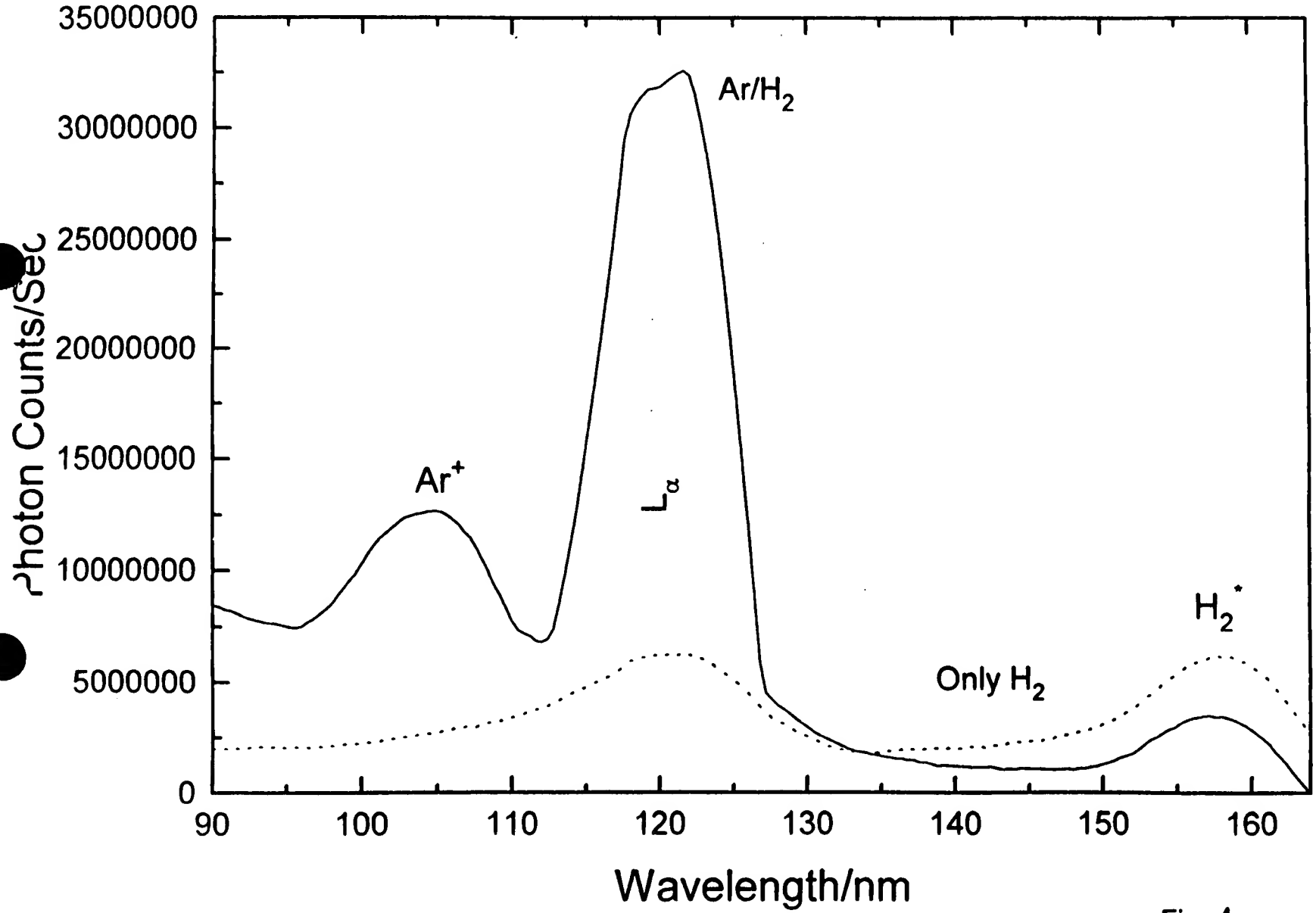
35000000
30000000
25000000
20000000
15000000
10000000
5000000
0
Photon Counts/Sec
90
100
110
120
130
140
150
160
Wavelength/nm
Ar/H2
Ar+
Lα
H2*
Only H2

Fig. 4

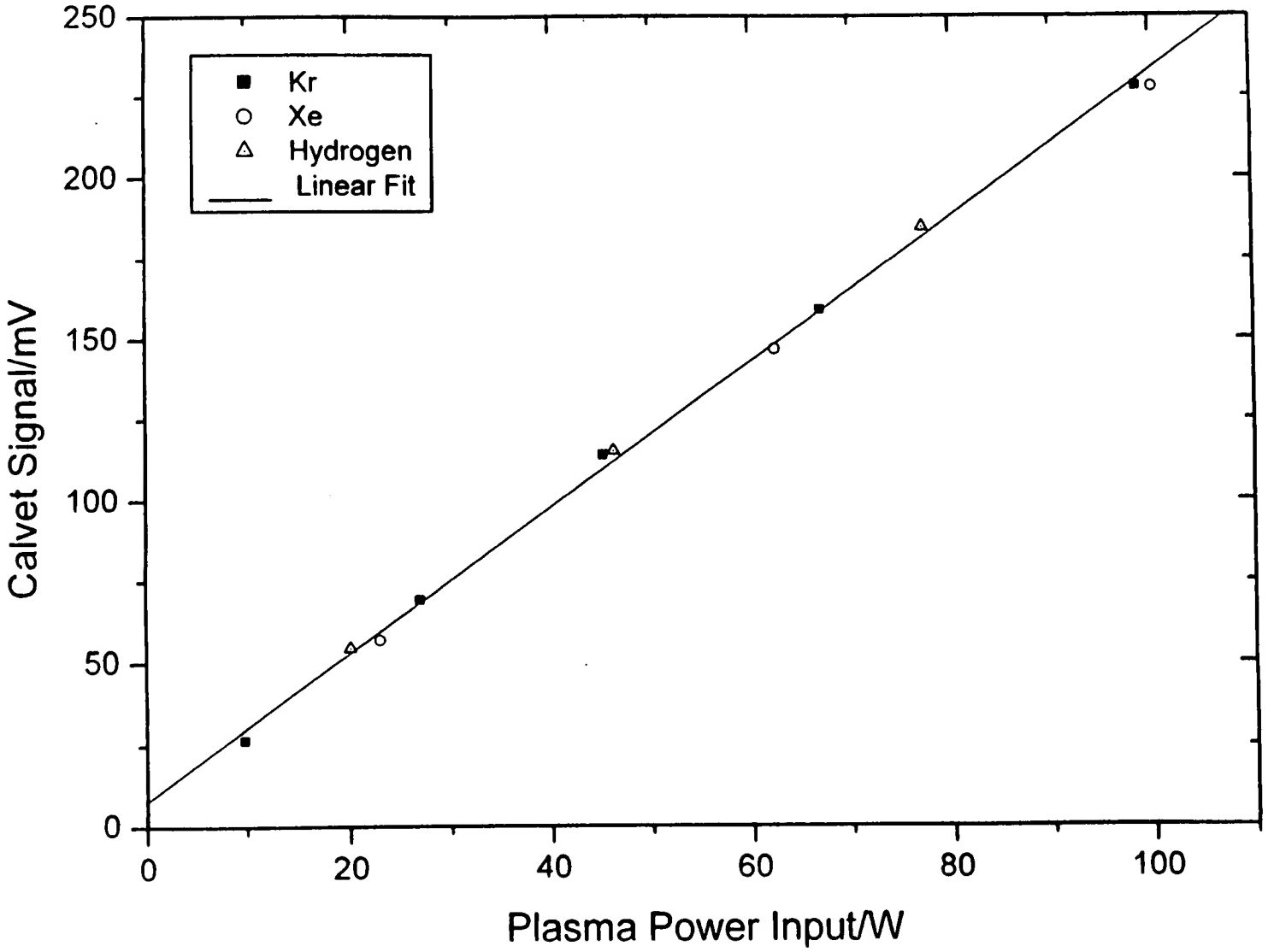
Kr
Xe
Hydrogen
Linear Fit
Calvet Signal/mV
Plasma Power Input/W
0
50
100
150
200
250
0
20
40
60
80
100

Fig. 5

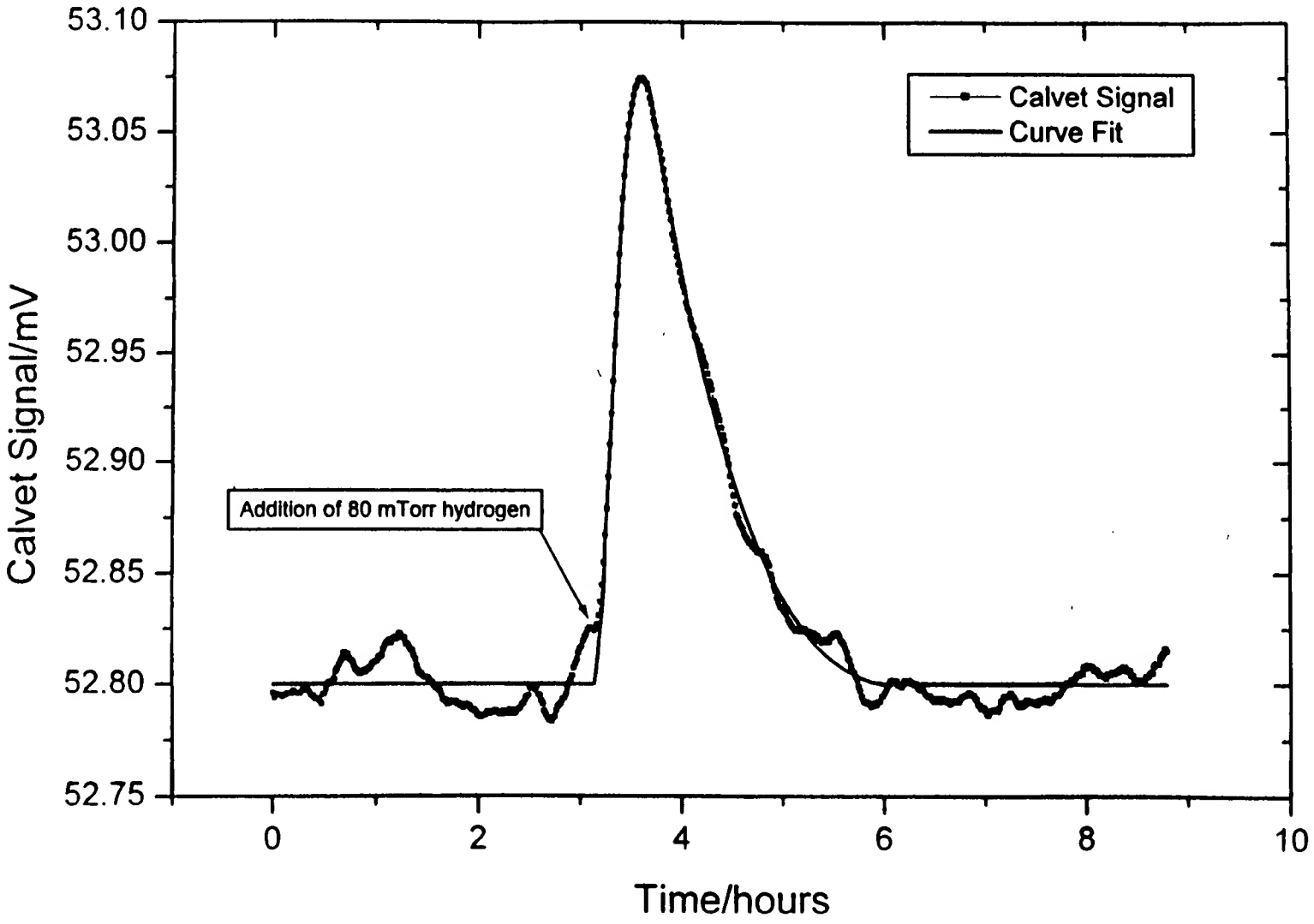
Calvet Signal
Curve Fit
Addition of 80 mTorr hydrogen
Calvet Signal/mV
Time/hours
53.10
53.05
53.00
52.95
52.90
52.85
52.80
52.75
0
2
4
6
8
10

Fig. 6

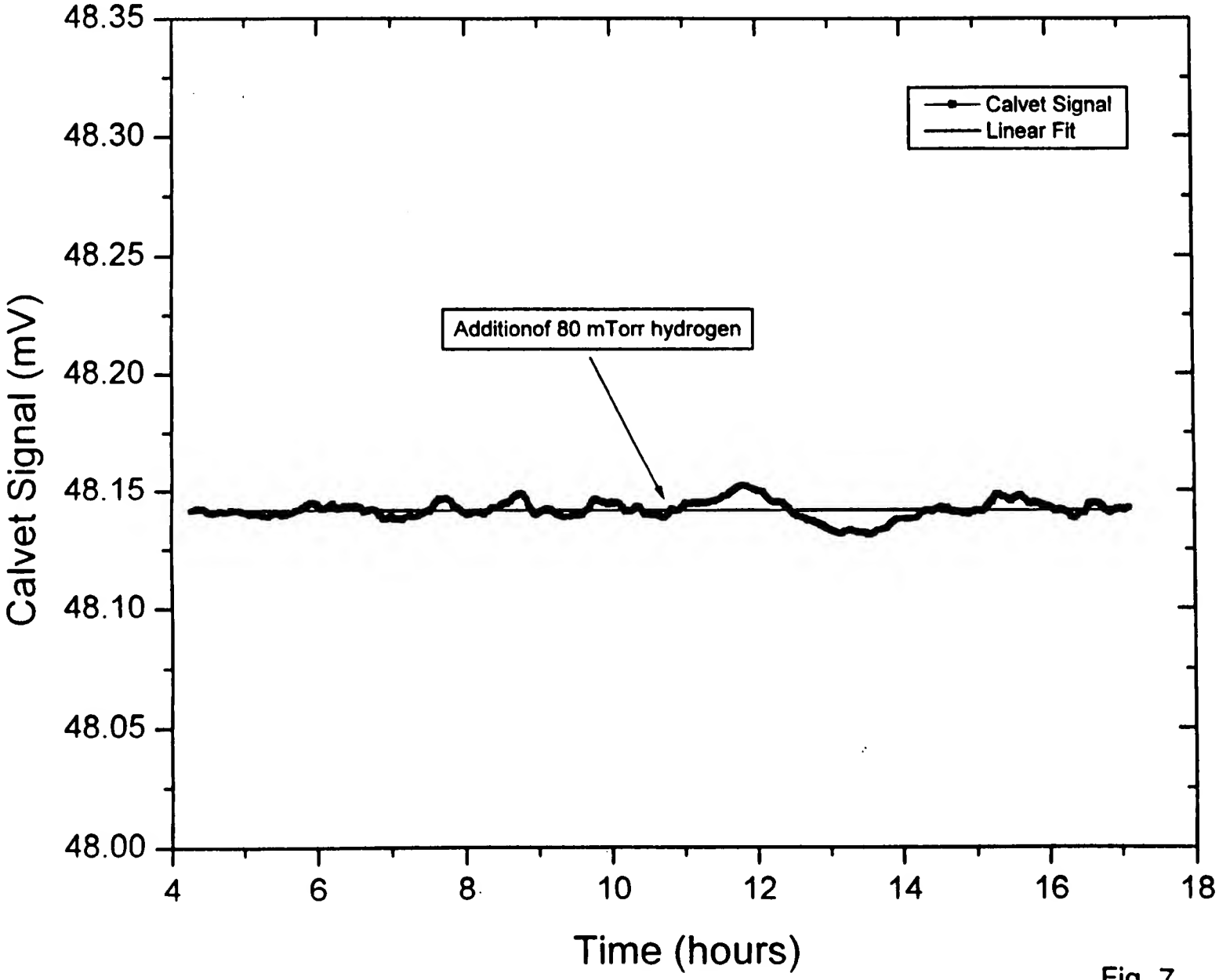
48.35
48.30
48.25
48.20
48.15
48.10
48.05
48.00
Calvet Signal (mV)
4
6
8
10
12
14
16
18
Time (hours)
Calvet Signal
Linear Fit
Additionof 80 mTorr hydrogen

Fig. 7